VERSITA

Chemical Papers 63 (6) 704–708 (2009)
DOI: 10.2478/s11696-009-0075-x

ORIGINAL PAPER

Novel use of silicon nanocrystals and nanodiamonds in biology‡

[a,b,c]Anna Fucikova*, [a]Jan Valenta, [b]Ivan Pelant, [c]Vitezslav Brezina

[a] *Faculty of Mathematics and Physics, Charles University, Ke Karlovu 3, 121 16 Prague 2, Czech Republic*

[b] *Institute of Physics AS CR, v.v.i., Cukrovarnicka 10, 162 53 Prague 6, Czech Republic*

[c] *Institute of Systems Biology and Ecology AS CR, v.v.i., Zamek 136, 373 33 Nove Hrady, Czech Republic*

Received 11 November 2008; Revised 20 May 2009; Accepted 21 May 2009

The presented work is aimed at the development of nontoxic nanocrystalline silicon fluorescence labels, biodegradable in living body and long-term stable, and of fluorescent nanodiamonds mainly for in vitro use. These novel fluorescence labels could be very good substitutes for commercially used quantum dots (e.g. cadmium compound quantum dots) which can be toxic according to the latest results. In this work, manufacturing of porous nanocrystalline silicon (por-Si) is described, several basic optical properties of por-Si are presented and the influence of Si nanocrystals, nanodiamonds, and milled silicon on the growth of a cell culture of L929 mouse fibroblast and HeLa cells is compared. Bio-interaction of nanoparticles was studied by optical transmission microscopy, time-lapse microphotography of cell culture evolution, fluorescence microscopy, fluorescence micro-spectroscopy, and scanning electron microscopy. The size and shape of nanocrystals were determined using atomic force microscopy (AFM).

Keywords: silicon nanocrystals, nanodiamonds, biocompatibility, quantum dot, fluorescence label, micro-spectroscopy

Introduction

First report on photoluminescence (PL) of porous silicon (por-Si) appeared in 1990 (Canham, 1990). It initiated extensive investigation of light-emitting silicon nanostructures with high application potential. Light-emitting silicon nanocrystals (Si-NCs) have a crystalline core of the size between 1–5 nm and their surface is most often covered by SiO_2. The PL properties depend not only on the Si-NC size but the surface of nanocrystal also plays a crucial role. Several PL emission bands of Si nanocrystals ranging from ultraviolet to near infrared spectral regions are described in literature. We are mostly interested in the yellow-orange luminescence band with slow stretched-exponential decay (lifetime of excited state 10–100 μs at room temperature). There are several models explaining the microscopic origin of the efficient PL of Si-NC (Canham, 1990; Valenta et al., 2008).

The second material studied in this work was nanocrystalline diamond which exhibits luminescence over the whole visible range of the electromagnetic spectrum in dependence upon various dopings. Nanodiamonds have a core of around 8 nm with its surface covered by various carboxy-, keto-, hydroxyl-, and oxygen groups (Eidelman et al., 2005). Nanodiamonds can be functionalized after silanization and they can be used e.g. in various bio-studies in cells (Vial et al., 2008; Osawa, 2005).

*Corresponding author, e-mail: anna.fucikova@mff.cuni.cz
‡Presented at the 1st Nanomaterials and Nanotechnology Meeting, Nano Ostrava, Ostrava, Czech Republic, 1–4 September 2008.

Material and methods

Preparation of nanoparticles

Por-Si was obtained by electrochemical etching of p-type [100] Si wafers, doped with boron to decrease the resistivity to 0.075–0.100 Ω cm. The etching solution consisted of hydrofluoric acid, hydrogen peroxide, and ethanol. The etching current density was set to 2.6 mA cm^{-2} to obtain fine porosity and size of nanocrystals between 2–5 nm (for the theoretical background see (Ossicini et al., 2003)). The freshly etched wafer was dipped into hydrogen peroxide for 5–10 min. The etched wafer with a por-Si layer on its surface was left to age for 12–48 h in a chamber with controlled temperature and air humidity. Por-Si powder (i.e. mixture of Si-NCs) was obtained by mechanical pulverization of the por-Si film from the Si wafer.

Rough powder of Si crystallites was prepared by dry milling of small pieces of Si wafer in a ball mill. The powder was mixed with deionized water and sedimented in order to remove big crystallites. The resulting size distribution had the peak at around 1 μm (< 80 vol. %), the size of microcrystals was determined by SEM experiments.

Nanodiamonds were prepared by combustion and then purified using acids (Osawa, 2005). Our samples were produced by NanoCarbon UDD-TAH, Diamond Centre, St. Petersburg, Russia. The product consisted of a mixture of 10 nm (56.6 vol. %) and 460 nm (43.4 vol. %) diamonds in deionized water, the size being measured by dynamic light scattering (DLS). After three days of sedimentation, an upper transparent part was formed. Only nanodiamonds with sizes of 10 nm were left in this supernatant, so they could be easily separated from the precipitate consisting of 460 nm diamonds. In case of biological studies, the supernatant part of the suspension was mixed into biological nutrient media.

Characterization of por-Si and nanodiamods

The por-Si powder was mixed with various solvents (preferentially ethanol, water, and xylene). In order to eliminate huge aggregates of interconnected nanocrystals, the colloid was left to settle for a few hours (up to two days) and the supernatant of the sedimented colloidal suspension was used in further experiments.

The photoluminescence emission and excitation spectra of por-Si colloidal suspensions were measured with a fluorescence spectrometer FluoroMax®-3. Spectra were corrected for the solvent influence (Raman scattering, impurities). Luminescence of por-Si grains (possibly down to single nanocrystals) was studied by a PL micro-spectroscopy apparatus consisting of an optical microscope Olympus IX-71, an imaging spectrograph SpectraPro 2150i, and a liquid-nitrogen-cooled CCD camera Spec-10 from Princeton Instruments. The sample was excited by a laser beam (458 nm from Ar-ion laser) through the objective (epifluorescence) or directly. For some measurements, the diluted suspension of Si-NCs was deposited on a quartz prism and excited by an evanescent wave of a laser beam totally reflected inside the prism.

The size of por-Si nanocrystals was studied using an AFM microscope (Agilent 5500 AFM/SPM Microscope) by depositing a highly diluted suspension on the HOPG graphite (Valenta at al., 2008) and analyzing the nanocrystal dimensions using oscillating mode AFM (AAC mode; 3 N m^{-1} spring constant and 60 kHz resonance frequency cantilevers from Nanosensors, Switzerland).

Interaction of nanostructures with cell cultures

Powder of the nanomaterials was sterilized by illumination with a UV lamp (254 nm) for 25 min and then added to a standard nutrient solution for each cell line (L929 mouse fibroblast and HeLa cells). The nutrient solution for L929 consisted of: 92 % MEM with Eagle stealth, 5 % newborn calf serum, 1 % antibiotics and antimicotics, 1 % L-glutamine, 1 % $NaHCO_3$. For HeLa cells, the nutrient solution consisted of: 86 % EMEM, 10 % newborn calf serum, 1 % antibiotics and antimicotics, 1 % L-glutamine, 1 % non essential amino acids, 1 % $NaHCO_3$ (all components from PAA company). The evolution of cell cultures with and without the addition of nanomaterials was studied by optical transmission microscopy, time-lapse, fluorescence microscopy, micro-spectroscopy, and scanning electron microscopy (SEM). In case of fluorescence observation of Si-NCs and nanodiamonds in biological samples, a safe excitation wavelength not inducing irreversible damage to cell cultures had to be used (Veselská & Janisch, 2000). The shortest safe wavelength of 360 nm was chosen.

Results and discussion

The AFM image (Fig. 1) shows that Si-NCs samples with the PL peak at around 600 nm contains nanocrystals with the diameter of approximately 2 nm (Valenta et al., 2008), nanocrystals prepared with an only slightly modified method exhibit the size of approximately 2.7 nm (HRTEM) (Dohnalová et al., 2008). Such nanocrystals are well suited to be used as labels in bio-environment, because animal cells do not have strong autofluorescence in this range of the optical spectrum.

The PL lifetime was found to be $\tau \sim 30$ μs at the emission wavelength of 600 nm for por-Si (maximum PL at around 600 nm) in ethanol (Fučíková et al., 2007). This relatively long PL decay time can be in principle used to differentiate the faster autofluorescence of cells from the slower PL of the por-Si labels

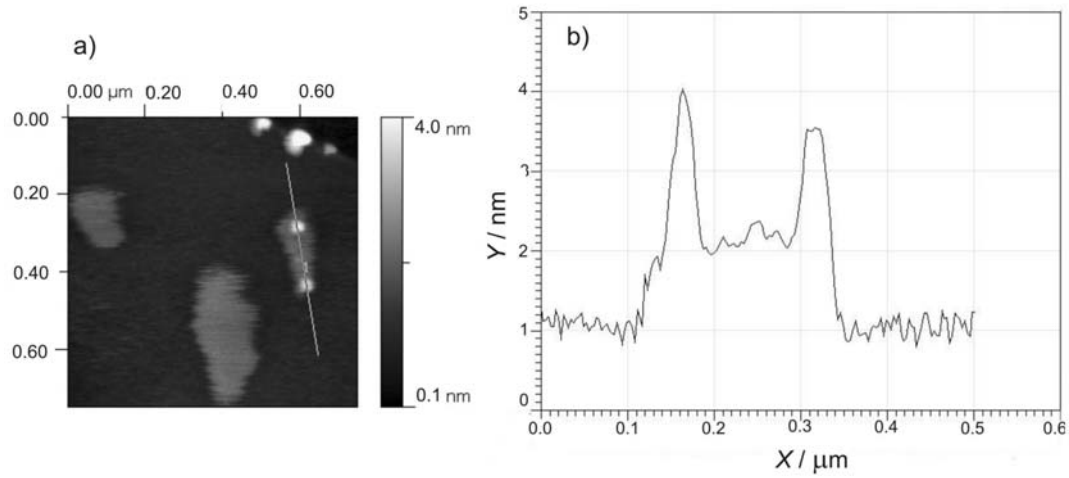

Fig. 1. (a) AFM image of 750 nm × 750 nm area of HOPG surface with several Si nanocrystals. (b) Profile taken along the white line. (The size of nanoparticles (∼2 nm) can be obtained from the height of peaks, while the lateral dimension of peaks is much larger than the real size of particles due to convolution with the AFM tip shape).

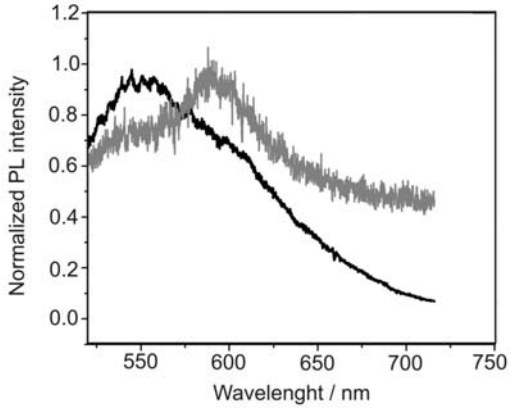

Fig. 2. PL spectra of several nanocrystal grains (passivated with SiO_2) in L929 cells (grey line) and in ethanol (black line). Excited with 325 nm from a continual wave Argon ion laser.

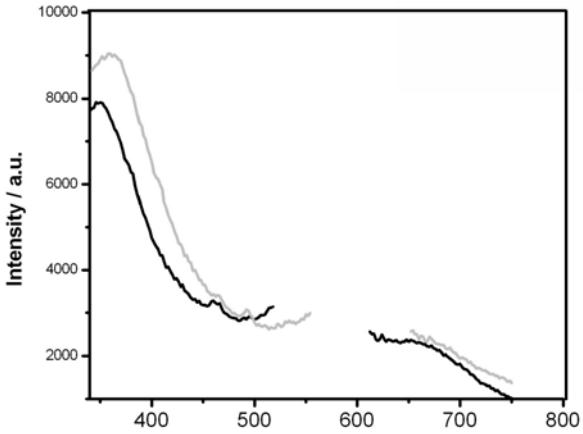

Fig. 3. PL spectra of nanodiamond colloidal suspension in water under various excitations wavelengths, λ: 280 nm (black line) and 300 nm (grey line).

when pulsed excitation and time correlated detection are used.

A small shift of the PL spectra of por-Si in cells was observed (Fig. 2) using the micro-spectroscopy set-up. The position of por-Si inside the cell was proved by z-scanning (changing the focal plane of the objective in vertical z-axis). The surface of por-Si reacts with reactive chemicals in cells and it is probably capped by some of them. The exact mechanism of the surface influence on the PL peak position needs further investigation. No shift in the peak position was observed after adding por-Si to the pure nutrient solution without cells. A similar shift (see Fig. 2) of the luminescence peak was observed when por-Si was treated in xylene (Kůsová et al., 2008).

Nanodiamonds, according to the last results, emit in the visible part of the spectrum with a PL peak between 600–800 nm (Yu et al., 2005). PL spectra of our nanodiamond samples consisted of two wide emission bands in the UV and visible ranges (Fig. 3).

The evolution of cell cultures with and without nanostructures in the nutrient medium was observed by time-lapse microphotography. The number of cells was calculated from the sequence of images and plotted against time, Figs. 4a and 4b. This number of cells was counted from three different spots in one counting compartment, four different compartments were examined (altogether 12 measurements). For HeLa cells, Fig. 4b, the growth curves show that cultures containing por-Si and nanodiamonds evolve only slightly slower (difference in the growth from 5–10 % for HeLa cells) than in the control sample for the concentration of nanoparticles of about 1 µg in 1 mL of nutrient media. On the other hand, the 1 µm Si particles and micro-diamonds in high dosages caused considerable stress to cells (100 times higher than por-Si) and the observed cultures exhibited necrosis after a few hours. In case of L929 cells in Fig. 4a, the growth curves show

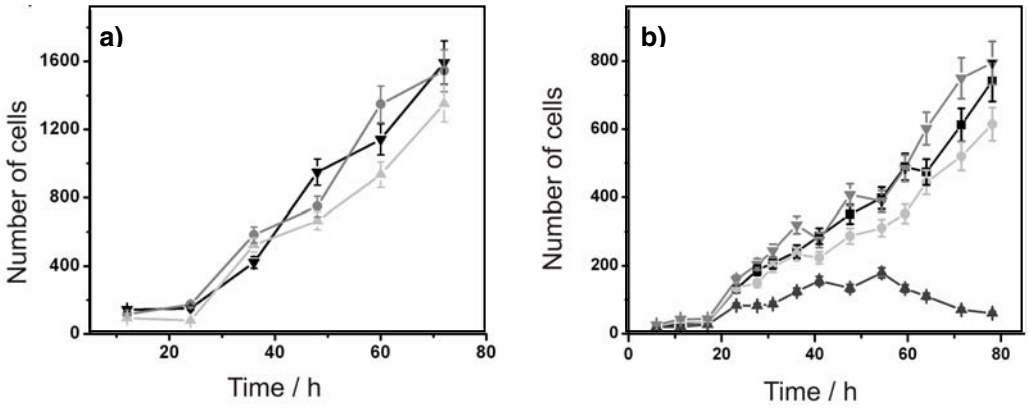

Fig. 4. (a) Grow curves of L929 cells incubated with por-Si (circles), milled Si (triangles up), and control (triangles down). (b) Grow curves of HeLa cells incubated with por-Si (circles), nanodiamonds (squares), control (triangles down), and high concentration of milled Si (triangles up).

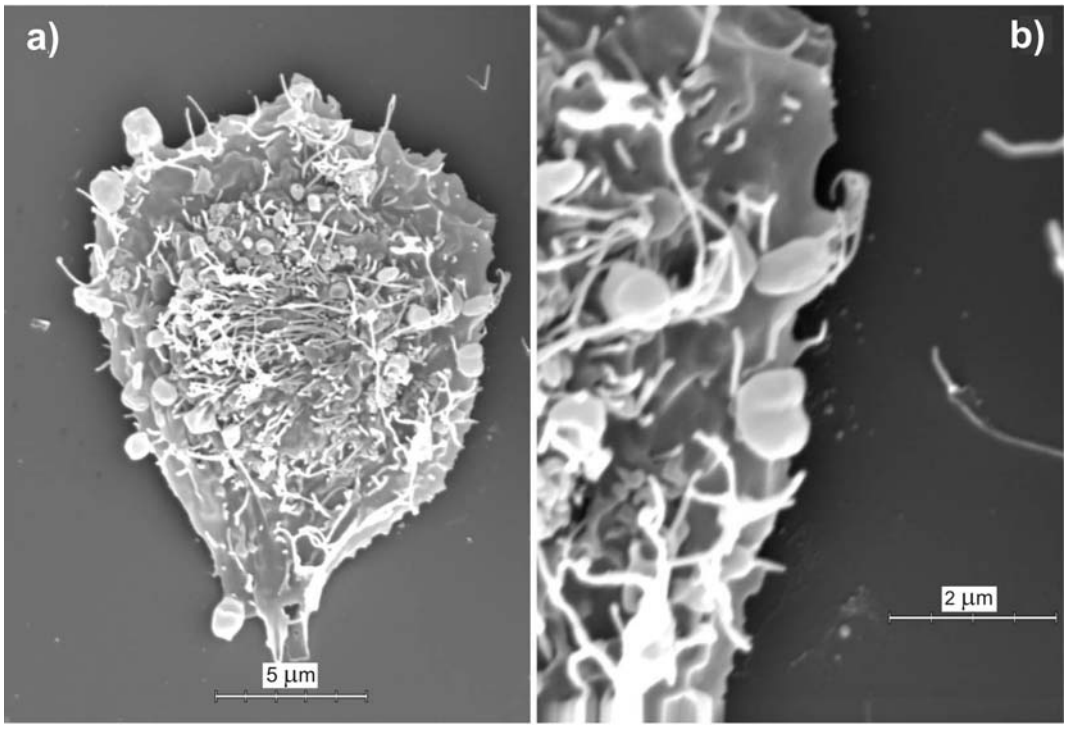

Fig. 5. (a) SEM of a cell of the L929 culture with high dosages of milled Si. (b) SEM detail of the L929 cell outer membrane with milled Si.

that cultures containing por-Si and 1 µm Si particles in very low dosages (10 times lower than por-Si) evolve without any noticeable difference in grow. The effect of nanodiamonds on the L929 cell line has not been studied yet.

It has to be noted that Si-NCs interacting with the medium tends to aggregate. This is due to a nonspecific interaction with the nutrient media. Growth of small floating clusters with time was observed; these clusters contain Si-NCs according to the results from fluorescence microscopy. Clustering was also observed when nanodiamonds were used but the presence of nanodiamonds on the surface of cells or inside them was not proved. When 1µm particles were studied, heavy clusters which did not move in the media were observed. This nonspecific binding could be overcome by a specific activation of the surface (Kumar, 2005). Optical (transmission and fluorescence) microscopy and SEM revealed that the maximal concentration of por-Si and 1µm particles is on the outer cell membrane (Figs. 5a and 5b), however, some por-Si particles were observed also inside the cell by fluorescence microscopy. The presumable way of their entering the cell is phagocytosis.

Conclusions

A series of por-Si (nanocrystals of 2 nm to 6 nm) with different fluorescence spectra do not have significant negative effect on the evolution of the cell culture; the accuracy of growth curves is around 8 %. A precise study on the toxicity using biochemical assays is, however, needed as well as a comparison study with commercially used quantum dots. On the other hand, particles of about 1 μm (milled silicon or diamond micro-crystals) are toxic in high concentrations. If the cell culture is observed, meronecrosis can be seen being caused by strong mechanical stress of the outer cell membrane caused by the incorporation of microparticles.

Por-Si was also observed to have a mild negative effect on the evolution of the cell culture at very high concentrations (more than 5 μg in 1 mL of nutrient media), but the cells are viable and cell division proceeds normally – the next cell generation shows normal behavior. Nanodiamonds have less negative effect compared to that of por-Si described above (in case of HeLa cells). Fluorescence microscopy applied on orange emitting por-Si shows that por-Si grains are concentrated on cell membranes, however, their presence in the internal cell environment was also observed.

Optical properties described above show promising application potential of por-Si and nanodiamonds as fluorescent labels. The size of these nanoparticles is smaller than that of the commercially used CdS-based quantum dots (e.g. EviTag® of around 25 nm). The next step towards applicable fluorescent labels is the development of bioactivation procedures (Medintz et al., 2005; Murcia & Neumann, 2005) and technology for large scale production of por-Si and nanodiamond particles.

Acknowledgements. This work was supported by the Czech Ministry of Education, Youth and Sports through the Research Centre LC510; project No. 202/07/0818 GAČR; the research plan MSM0021620835 and the Institutional Research Plan No. AV0Z 10100521, KAN400100701 (GAAV), and GAUK 101008. Many thanks for experimental assistance and advice to A. Kromka, B. Rezek, G. Kada, K. Kůsová, K. Dohnalová, and K. Žídek and for the DLS measurement to C. Konak, Institute of Macromolecular Chemistry, Academy of Sciences of the Czech Republic, v.v.i., Prague, Czech Republic.

References

Canham, L. T. (1990). Silicon quantum wire array fabrication by electrochemical and chemical dissolution of wafers. *Applied Physics Letters*, *57*, 1046–1048. DOI: 10.1063/1.103561.

Dohnalová, K., Pelant, I., Kůsová, K., Gilliot, P., Gallart, M., Crégut, O., Rehspringer, J.-L., Hönerlage, B., Ostatnický, T., & Bakardjeva, S. (2008). Closely packed luminescent silicon nanocrystals in a distributed-feedback laser cavity. *New Journal of Physics*, *10*, 063014. DOI: 10.1088/1367-2630/10/6/063014.

Eidelman, E. D., Siklitsky, V. I., Sharonova, M. A., Yagovkina, A., Vul', A. Ya., Takahashi, M., Inakuma, M., Ozawa, M., & Osawa, E. (2005). A stable suspension of single ultrananocrystalline diamond particles. *Diamond and Related Materials*, *14*, 1765–1769. DOI: 10.1016/j.diamond.2005.08.057.

Fučíková, A., Valenta, J., Pelant, I., & Březina, V. (2007). Studies of nanocrystalline silicon colloidal suspensions and their interaction with a biological system. *Acta Metallurgica Slovaca*, *13*, 88–92.

Kumar, C. S. S. R. (Ed.) (2005). *Biofunctionalization of nanomaterials*. Weinheim, Germany: Wiley–VCH.

Kůsová, K., Cibulka, O., Dohnalová, K., Pelant, I., Fučíková, A., & Valenta, J. (2008). Yellow-emitting colloidal suspensions of silicon nanocrystals: Fabrication technology, luminescence performance and application prospects. *Physica E*, *41*, 982–985. DOI: 10.1016/j.physe.2008.08.02.

Medintz, I. L., Uyeda, H. T., Goldman, E. R., & Mattoussi, H. (2005). Quantum dot bioconjugates for imaging, labelling and sensing, *Nature Materials*, *4*, 435–446. DOI: 10.1038/nmat1390.

Murcia, M. J., & Neumann, C. A. (2005). Biofunctionalization of fluorescent nanoparticles. In C. S. S. R. Kumar (Ed.), *Biofunctionalization of nanomaterials* (pp. 1–40). Weinheim, Germany: Wiley–VCH.

Osawa, E. (2005). Disintegration and purification of crude aggregates of detonation nanodiamond. A few remarks on nano methodology. In D. M. Gruen, O. A. Shenderova, & A. Ya. Vul' (Eds.), *Synthesis, properties and applications of ultrananocrystalline diamond* (pp. 231–240). Dordrecht, The Netherlands: Springer.

Ossicini, S., Pavesi, L., & Priolo, F. (2003). *Light emitting silicon for microphotonics*. Berlin/Heidelberg, Germany: Springer.

Valenta, J., Fučíková, A., Pelant, I., Kůsová, K., Dohnalová, K., Aleknavičius, A., Cibulka, O., Fojtík, A., & Kada, G. (2008). On the origin of the fast photoluminescence band in small silicon nanoparticles. *New Journal of Physics*, *10*, 073022. DOI: 10.1088/1367-2630/10/7/073022.

Veselská, R., & Janisch, R. (2000). The effect of UV irradiation on changes in cytoskeleton and viability of mouse fibroblast L929 cell line. *Scripta Medica*, *73*, 393–408.

Vial, S., Mansuy, C., Sagan, S., Irinopoulou, T., Burlina, F., Boudou, J.-P., Chassaing, G., & Lavielle, S. (2008). Peptide-grafted nanodiamonds: preparation, cytotoxicity and uptake in cells. *ChemBioChem*, *9*, 2113–2119. DOI: 10.1002/cbic.200800247.

Yu, S.-J., Kang, M.-W., Chang, H.-C., Chen, K.-M., & Yu, Y.-C. (2005). Bright fluorescent nanodiamonds: No photobleaching and low cytotoxicity. *Journal of the American Chemical Society*, *127*, 17604–17605. DOI: 10.1021/ja0567081.